Time-Dependent Characteristics of Sulfonated EPDM Containing Zinc Stearate. I. Thermal Behavior

R. A. WEISS, *Institute of Materials Science and Department of Chemical Engineering, University of Connecticut, Storrs, Connecticut 06268*

Synopsis

The crystallization and melting of zinc stearate (ZnSt) in ZnSt-plasticized compositions of ethylene–propylene–diene terpolymer (EPDM) and sulfonated EPDM (S-EPDM) have been studied by differential scanning calorimetry. While immiscible in both EPDM and S-EPDM, ZnSt is compatible with the latter. This compatibility presumably arises from either electrostatic or dipole–dipole interactions between the carboxylate functionality of ZnSt and the sulfonate groups of the polymer. The crystallization behavior of ZnSt is significantly perturbed when the material is added to S-EPDM, and the crystalline ZnSt phase that results is strongly time dependent. ZnSt first crystallizes as small imperfect crystals when the compositions are cooled from the melt, but it eventually anneals at room temperature into larger, more perfect crystals. Time dependent changes in the mechanical properties of these compositions are also demonstrated and it is suggested that this may be due in part to changes in the ZnSt morphology.

INTRODUCTION

The interest in ion-containing polymers, ionomers, has grown considerably over the past decade. These materials have been the subject of several books[1–3] and a recent review article.[4] The unique characteristics of ionomers arise from intermolecular coulombic interactions between the ionic species. This *ionic crosslink* results in physical properties characteristic of covalently crosslinked polymers. The ionic crosslink is not, however, permanent; ionomers can be dissolved in suitable solvents and exhibit viscous flow at elevated temperatures.

One particular ionomer that has received considerable attention in recent years is sulfonated ethylene–propylene–diene terpolymer, S-EPDM.[5–18] Interactions between sulfonate groups give rise to a strongly associated network structure at room temperature; yet at elevated temperatures the ionic associations relax sufficiently to allow for melt processability by conventional techniques, e.g., extrusion and injection molding. For this reason, this ionomer has been considered for commercial applications as a thermoplastic rubber.

One deficiency of S-EPDM is its extremely high melt viscosity at normal processing temperatures, which renders use of the neat resin impractical. It is possible, however, to achieve significant reductions in the melt viscosity by the addition of various polar additives that interact preferentially with the ionic associations.[8] While these additives, termed *ionic-domain plasticizers*, are effective at lowering the melt viscosity, they also, in general, have a detrimental effect on the mechanical properties of the ionomer.

One particular ionic-domain plasticizer, zinc stearate (ZnSt), not only improves the melt flow of S-EPDM, but also improves the mechanical properties of the

Journal of Applied Polymer Science, Vol. 28, 3321–3332 (1983)
 CCC 0021-8995/83/113321-12$02.20

resultant system.[10] The improvement of the melt flow at elevated temperatures is due to the preferential solvation of the sulfonate associations by ZnSt that weakens the crosslink structure. The improvement of the tensile strength is believed to result from the formation of a separate crystalline ZnSt phase that strongly interacts with the metal sulfonate groups. It is worth noting that the behavior of ZnSt in S-EPDM is markedly different from its behavior in unsulfonated EPDM. In the latter system, ZnSt exudes from the polymer. On the other hand, ZnSt appears to be stable in S-EPDM, though it does exist as a separate crystalline microphase as evidenced by the presence of a melting endotherm by differential scanning calorimetry (DSC).

In this paper, we will discuss the crystallization and melting phenomena of ZnSt in both EPDM and S-EPDM at various plasticizer concentrations. Particular attention will be given to time-dependent effects. In a future publication we will describe the corresponding time-dependent behavior of the mechanical properties of these systems.

EXPERIMENTAL

The EPDM, S-EPDM, and ZnSt-filled S-EPDM's containing up to 50% (wt) ZnSt were supplied by Dr. Ilan Duvdevani of the Exxon Research and Engineering Co. The EPDM had a composition of 55% ethylene, 40% propylene, and 5% ethylidene norborene and a 20 Mooney viscosity (20 M_L at 100°C). The S-EPDM was prepared by the sulfonation of EPDM with acetyl sulfate followed by neutralization with zinc acetate,[19] and it contained 30 meq of zinc sulfonate. Compounds of S-EPDM with ZnSt were prepared on a heated two-roll mill using conventional rubber compounding techniques. ZnSt-filled EPDM samples containing up to 50% (wt) ZnSt were prepared by dissolution of the components in toluene followed by precipitation in methanol and drying under vacuum at ca. 50°C.

Thermal analyses were made with a Perkin-Elmer DSC-2 equipped with a low temperature cooling accessory and interfaced with a Perkin-Elmer Data Station, Model 3500. All samples were crimped inside aluminum pans and measurements were made in either a dry nitrogen or helium atmosphere. Temperature and energy calibrations were performed with indium, water, and cyclohexane. Unless otherwise noted, all heating and cooling scans were obtained at 20 K/min. The

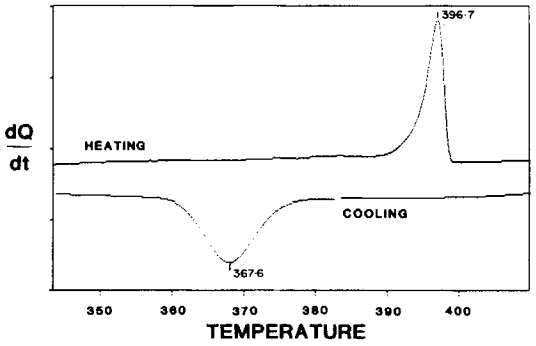

Fig. 1. DSC thermograms for the zinc stearate used: (top) heating and (bottom) cooling.

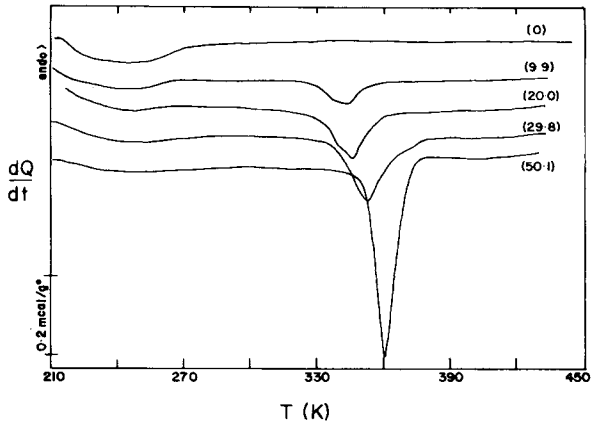

Fig. 2. DSC cooling thermograms for ZnSt/EPDM blends. Numbers in parentheses correspond to weight percent ZnSt in sample.

melting and crystallization temperatures reported represent peak temperatures (i.e., maximum rate of melting or crystallization) and the heat of fusion or crystallization values were determined by the standard Perkin-Elmer thermal analysis software for the Data Station.

Dynamic moduli measurements were made at 36°C with a Rheometrics Mechanical Spectrometer using oscillating parallel plates and a frequency of 0.1 Hz. The strain amplitude was chosen so as to be within the region of linear viscoelasticity.

RESULTS AND DISCUSSION

The heating and cooling curves for the zinc stearate used are shown in Figure 1. The melting endotherm is depressed from that of pure ZnSt, ca. 130°C,[20] and shows a low temperature shoulder that indicates that this material contains some impurity, probably stearic acid. No attempts were made to purify the ZnSt.

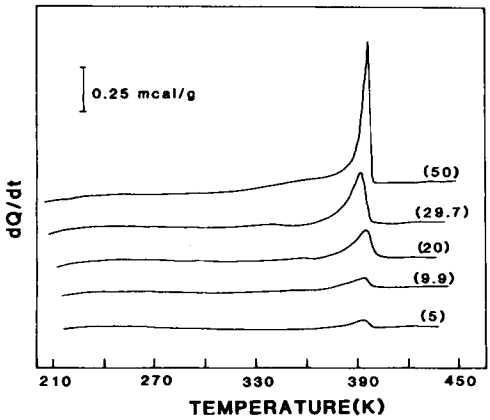

Fig. 3. DSC heating thermograms for ZnSt/EPDM blends run immediately after cooling sample from the melt at 20 K/min. Numbers in parentheses correspond to weight percent ZnSt in sample.

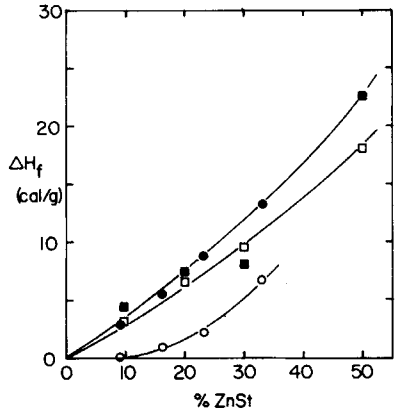

Fig. 4. Heat of fusion for ZnSt/EPDM (□,■) and ZnSt/S-EPDM (○,●) blends: (□,○) samples heated immediately after cooling from the melt; (■,●) well-aged samples.

Figures 2 and 3 show the cooling scan and the subsequent heating scan for various samples of EPDM containing ZnSt. Visual observations of these materials indicated that the two components were immiscible and incompatible in the solid state. Solid samples were cloudy indicating that there were two phases, and ZnSt eventually diffused to the surface. The DSC cooling thermograms (Fig. 2), show a single crystallization exotherm that occurs at decreasing temperature with decreasing ZnSt concentration. Since EPDM exhibits no exothermic activity in identical experiments, this exotherm can be attributed to crystallization of a ZnSt phase. The heating thermograms obtained immediately after the cooling scans (Fig. 3) show a single melting endotherm at a temperature that decreases and broadens with decreasing ZnSt concentration. There is a hint of a slightly lower temperature endotherm in the samples containing the highest ZnSt concentration that most likely corresponds to the low temperature shoulder observed in the heating thermogram of the pure ZnSt (cf. Fig. 1).

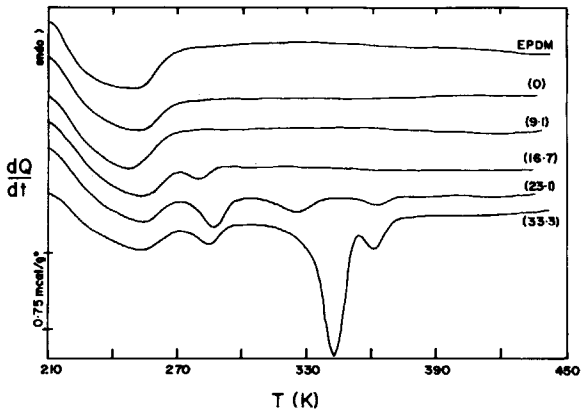

Fig. 5. DSC cooling thermograms for ZnSt/S-EPDM blends. Numbers in parentheses correspond to wt % ZnSt in sample.

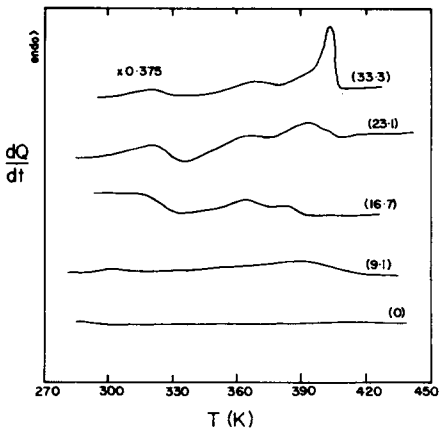

Fig. 6. DSC heating thermograms of ZnSt/S-EPDM samples run immediately after cooling sample from the melt at 20 K/min. Numbers of parentheses correspond to wt % ZnSt in sample.

After aging the ZnSt/EPDM samples, the melting characteristics of the ZnSt phase change slightly. The heat of fusion calculated by integrating under the endotherm (see Fig. 4) and the temperature corresponding to the maximum rate of melting increase with time. For the lower ZnSt concentrations the melting endotherm of ZnSt resolves into a double peak. Within experimental error, all the ZnSt was accounted for in the melting endotherms of the aged samples. These results are consistent with the observation of phase separation in these samples; that is, as the ZnSt diffuses out of the sample, one would expect the melting temperature to increase, since the ZnSt crystals most likely increase in size and perfection. The time dependence of ΔH_f indicates that some ZnSt is miscible in the EPDM at high temperature and does not crystallize as the sample is cooled from the melt. The fraction of ZnSt that does not crystallize during the cooling experiment, however, is apparently immiscible in EPDM at room temperature and eventually does phase separate and crystallize.

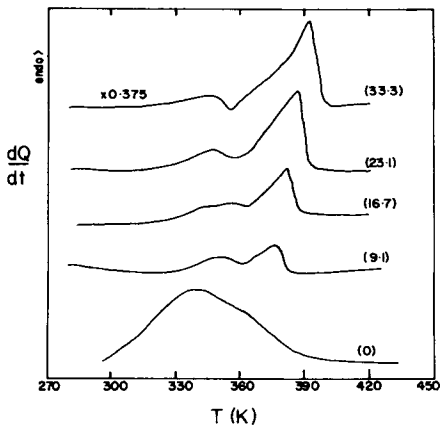

Fig. 7. DSC heating thermograms of well-aged ZnSt/S-EPDM samples. Numbers in parentheses correspond to wt % ZnSt in sample.

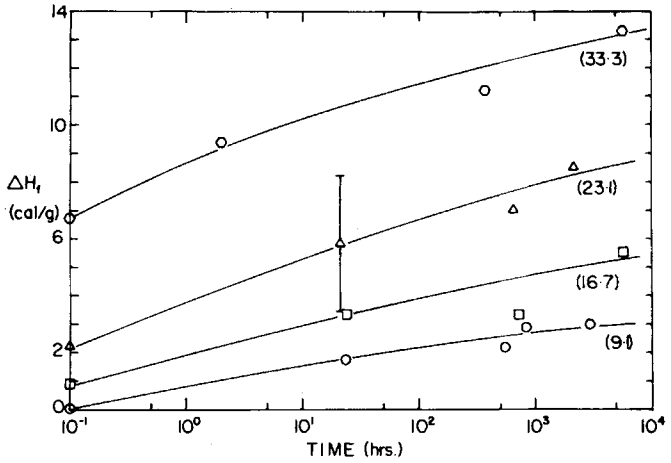

Fig. 8. Heat of fusion as a function of time after cooling sample from the melt for various concentrations of ZnSt in S-EPDM (numbers in parentheses correspond to wt % ZnSt).

Whereas ZnSt is incompatible with EPDM, it is compatible with S-EPDM at all concentrations considered in this study. Compatible is taken here to mean that no macroscopic phase separation occurs. The ZnSt is, however, immiscible or only partly miscible in S-EPDM. This is evidenced by the detection of crystallization and melting of a ZnSt phase by DSC (Figs. 5–7). Although the two components are immiscible, these materials are relatively clear, which indicates that the dispersed ZnSt phase is sufficiently small so as not to scatter visible light.

The cooling thermograms of the ZnSt/S-EPDM samples are distinctly different from the corresponding ZnSt/EPDM materials (cf. Figs. 2 and 5). A crystallization exotherm is observed only in samples with greater than 9.1% (wt) ZnSt, and multiple exotherms are observed for the higher ZnSt concentrations. The large supercoolings observed indicate the formation of small imperfect ZnSt crystals, which is consistent with the lack of light scattering by the samples.

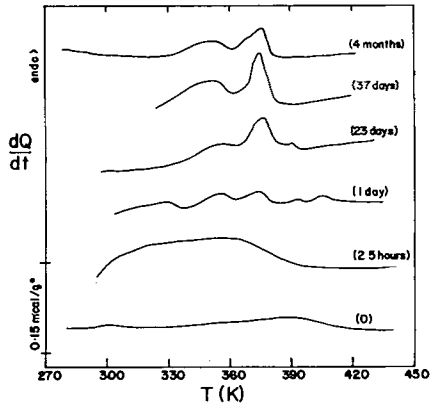

Fig. 9. DSC heating thermograms of S-EPDM containing 9.1% ZnSt as a function of aging time at room temperature.

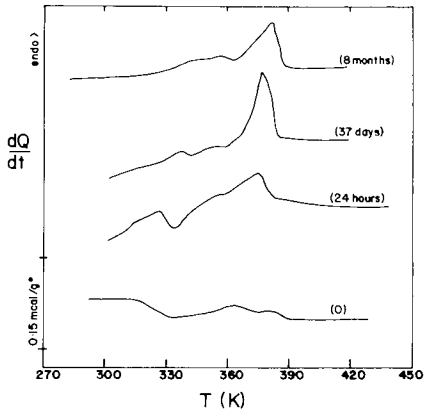

Fig. 10. DSC heating thermograms of S-EPDM containing 16.7% ZnSt as a function of aging time at room temperature.

Although no ZnSt crystallization is observed in the 9.1% ZnSt sample and little, if any melting is observed in the heating thermogram of the quenched sample (Fig. 6), subsequent heating thermograms after aging at room temperature indicate that at least some of the ZnSt eventually crystallizes (see Fig. 7). Although an endotherm is observed near 120°C in the heating thermogram for the quenched 9.1% ZnSt sample, this is not believed to be due to ZnSt crystallinity, as will be discussed later in this paper.

The heating scans of the quenched and aged ZnSt/S-EPDM samples, (Figs. 6 and 7) exhibit multiple endotherms, and the position and intensity of these endotherms are sensitive to the aging time. As with the ZnSt/EPDM samples, the ΔH_f of the ZnSt/S-EPDM samples increased with aging time, but for the latter the changes were much more dramatic (see Fig. 4). For example, for the 9.1% ZnSt/S-EPDM sample all of the ZnSt crystallizes after the sample is cooled, and, even for the 33% ZnSt sample, about 50% of the crystallization occurs during aging.

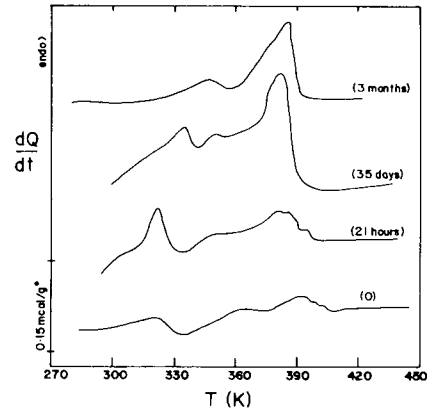

Fig. 11. DSC heating thermograms of S-EPDM containing 23.1% ZnSt as a function of aging time at room temperature.

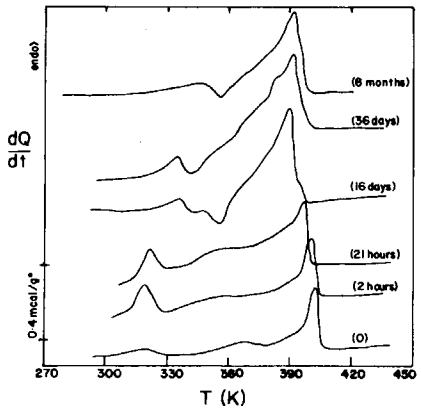

Fig. 12. DSC heating thermograms of S-EPDM containing 33.3% ZnSt as a function of aging time at room temperature.

The relationship between ΔH_f and aging time for the ZnSt/S-EPDM materials after cooling from the melt is given in Figure 8. Here it is seen that post-cooling crystallization occurs over an extremely long period of time, and, in fact, equilibrium is not reached even after 8 months. The error bar shown for the one datum point represents the range of ΔH_f values calculated for that sample and represents the worst case. The error in the ΔH_f measurements arises not from reproducibility of the data, but from uncertainty as to how to draw the baseline. Many of the DSC scans were complex and may have included exotherms as well as melting endotherms. This probably represents melting and recrystallization of ZnSt during the thermal analysis experiment, and, as a consequence, the ΔH_f values calculated from these thermograms may not accurately represent the amount of ZnSt crystallinity present before the analysis. Similarly, the data in Figure 8 may be misleading, but, even though the ΔH_f calculations may not be accurate, the sample is most certainly not at equilibrium.

The DSC heating thermograms of four representative ZnSt/S-EPDM samples as a function of aging time are shown in Figures 9–12. While it is difficult to characterize the changes that occur, two trends are apparent in all of the samples. For each ZnSt concentration three definite endotherms are observed. During aging the lowest temperature endotherm diminishes in intensity and increases in temperature. The highest temperature endotherm increases in intensity, but the temperature of this event remains constant. The intermediate endotherm does not exhibit any clear trend, and this may be due to the influence of the lowest temperature endotherm which appears to merge with the intermediate event. In general, the higher temperature endotherm becomes more distinct at the expense of the two lower events. These data suggest that the ZnSt crystals increase in size during aging, though conformation of this conclusion requires additional experimental evidence, such as microscopy. As mentioned earlier, many thermograms showed distinct exotherms (e.g., 33% ZnSt/S-EPDM at 16 days) that suggests that whatever melted at the lower temperature recrystallized and contributed to the melting endotherms observed at higher temperatures. Again, while any conclusions as to the ZnSt morphology must await further experimentation, three conclusions are definite: (1) the morphology of these materials

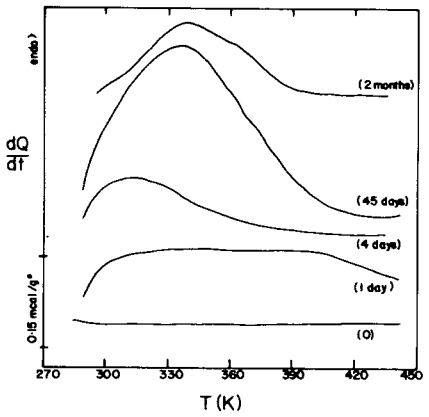

Fig. 13. DSC heating thermograms of S-EPDM as a function of aging time at room temperature.

is time-dependent; (2) there is a distribution of ZnSt crystal sizes as evidenced by the multiple thermal events; and (3) the complex nature of the ZnSt crystallization and melting is a direct result of some kind of interaction with the sulfonate group on the polymer. The latter conclusion is based on the absence of these complexities when EPDM is used. One might also speculate that the apparent compatibility of ZnSt and S-EPDM arises from the dipole–dipole or electrostatic interactions between the sulfonate and carboxylate groups. Similarly, as postulated earlier, it is these interactions that contribute to the ability of ZnSt to plasticize and reinforce the polymer.[10]

Recently, Maurer reported some anomalous thermal behavior of S-EPDM without ZnSt.[17] He observed that an endotherm appeared near 100°C in the DSC heating thermogram as the S-EPDM was aged at room temperature after being cooled from the melt. The endotherm first grew in intensity with time, but eventually decreased after several months. Maurer observed this endotherm in solution-cast, compression-molded, and fractionated samples.

The DSC heating thermograms of the S-EPDM used in this current study are shown in Figure 13 as a function of annealing time at room temperature. As with Maurer's experiments, an endotherm is observed with aging of the S-EPDM, and it increased in intensity up to ca. 45 days and then decreased in intensity. The temperature at which this event was observed, ca. 60°C, is lower than reported by Maurer, but this discrepancy may be due to differences in the EPDM molecular weight and sulfonate concentrations used in the two studies. The origin of this endotherm is unknown. Maurer suggested that it is a result of the formation of the ionic crosslink network, but this conclusion must be considered speculative without additional evidence. This endotherm may be an artifact due to changes in the sample shape as it is heated in the DSC. Because of the ionic crosslinks which may persist in the melt, there may be considerable internal stresses induced in the sample during compression molding. These should relax with time, and the DSC results shown here may be a consequence of different degrees of stress relief taking place.

What is even more puzzling are the data in Figure 14, DSC heating thermograms for the base-EPDM as a function of aging time. These samples were

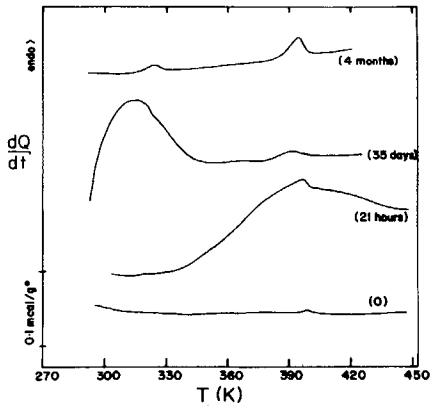

Fig. 14. DSC heating thermograms of EPDM as a function of aging time at room temperature.

compression-molded at room temperature. During aging an endotherm was observed near 120°C and grew in intensity over the first day and then decreased in intensity. After several days another endotherm, at ca. 50°C, was observed and it, too, increased, then decreased in intensity.

No definitive explanation can be given here for the thermal behavior of the EPDM and S-EPDM resins. Furthermore, it is not clear whether these *anomalous* thermal events were also present in the ZnSt-filled samples. If so, the superposition of this event and the ZnSt melting endotherm further complicate the determination of ΔH_f. The origin of this phenomenon requires additional studies of these polymers.

ZnSt is added to S-EPDM in order to plasticize the melt, and it is extremely effective at reducing the melt viscosity.[8] It has been postulated that the ZnSt interacts preferentially with the ionic phase, i.e., the sulfonate groups. Conventional plasticizers usually influence the solid state properties of a polymer,

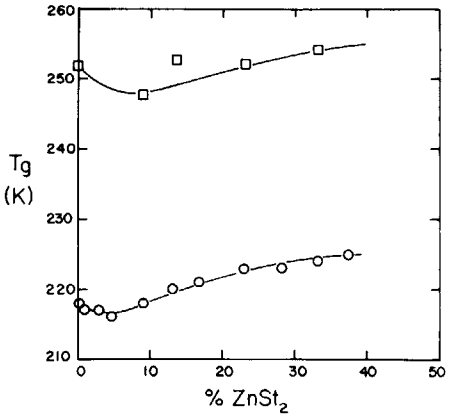

Fig. 15. Glass transition temperature of ZnSt/S-EPDM blends as a function of ZnSt concentration: (□) T_g defined as the maximum in the exotherm occurring nearing T_g in the cooling thermograms (see Fig. 6); (○) T_g defined as $\Delta c_p/2$ in the cooling temperature.

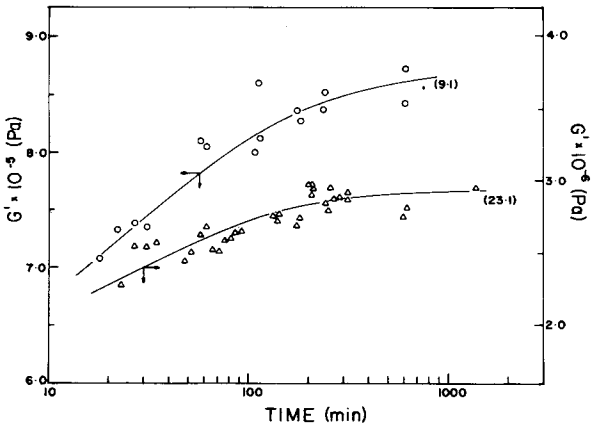

Fig. 16. Dynamic modulus of ZnSt/S-EPDM blends as a function of aging time: (○) 9.1% ZnSt; (△) 23.1% ZnSt.

by lowering the glass transition temperature T_g. If the ZnSt were associated with the sulfonate groups, the lowering of the T_g of the EPDM backbone by the addition of ZnSt would not be expected.

Measurement of the T_g of these materials by DSC was complicated by the presence of an exotherm during cooling in the vicinity of T_g (see Fig. 6). This exotherm was also observed in the neat S-EPDM and in the EPDM, and, while its origin is not clear, it may be due to some crystallization of short ethylene sequences in the EPDM. T_g's were estimated in two ways: (1) by taking $\Delta c_p/2$ from the low temperature baseline to the peak of the exotherm and (2) taking the peak temperature of the exotherm. While both of these methods are somewhat arbitrary, the error involved with these estimates of T_g is probably consistent from sample to sample. The resuls are shown in Figure 15, and in both cases the data show that T_g increases with increasing ZnSt. This result is consistent with the dynamic mechanical data of Agarwal et al.,[13] and the increase of T_g is probably due to interactions between the ZnSt phase and the sulfonate groups that act as physical crosslinks. This same explanation can be used to explain the increase in modulus that occurs in these materials by the addition of ZnSt. Figure 15 shows a small decline in T_g at low ZnSt loadings, and it is not clear at this time whether this decrease is real or whether it is a result of how T_g was calculated.

Part of the justification for this investigation was the observation that dramatic changes in the mechanical properties of these systems occur with time after being cooled from the melt. Figure 16 is a plot of the dynamic modulus vs. time for two ZnSt/S-EPDM samples. In both cases a greater than 20% increase in modulus occurs over a period of 16 h. This change in properties was heretofore thought to be due to changes in the sulfonate associations that occur in S-EPDM. This study suggests that some of these changes may be due to post-crystallization of the ZnSt, though the time scale for the property changes in Figure 16 is much smaller than that of the crystallization changes. The property and morphological changes of these materials will be considered in more detail in a future paper.

CONCLUSIONS

It has been demonstrated that zinc stearate, while immiscible in both EPDM and S-EPDM, is compatible with the latter. This compatibility arises from some kind of interaction between the stearate and the sulfonate groups of the polymer. The crystallization behavior of ZnSt is significantly perturbed when the material is added to S-EPDM and the ZnSt crystal phase that results is strongly time-dependent. The thermal analyses presented here indicate that ZnSt in S-EPDM first crystallizes into small imperfect crystals when cooled from the melt and subsequently anneals at room temperature into larger more perfect crystals. ZnSt-filled S-EPDM also exhibits time dependent mechanical properties, and this may be due in part to changes in the ZnSt crystal morphology.

This work was supported by grants from the National Science Foundation, Grant No. DMR-8108333, and by the University of Connecticut Research Foundation. Much of the experimental work was carried out by Ms. Inger Damon.

References

1. A. Eisenberg and M. King, *Ion-Containing Polymers*, Academic, New York, 1977.
2. L. Holliday, Ed., *Ionic Polymers*, Applied Science, London, 1975.
3. A. Eisenberg, Ed., *Ions in Polymers*, American Chemical Society, Washington, D.C., 1980.
4. W. J. MacKnight and T. R. Earnest, Jr., *J. Polym. Sci., Macromol. Rev.*, **16**, 41 (1981).
5. N. H. Canter, U.S. Pat. 3,642,728 (1974) (assigned to Esso Research and Engineering Co.).
6. C. P. O'Farrell and G. E. Sernvick, U.S. Pat. 3,836,511 (1974) (assigned to Esso Research and Engineering Co.).
7. H. S. Makowski, R. D. Lundberg, L. Westerman, and J. Bock, in *Ions in Polymers*, A. Eisenberg, ed., American Chemical Society, Washington, D.C., 1980, p. 3.
8. H. S. Makowski and R. D. Lundberg, in Ref. 7, p. 37.
9. D. Brenner and A. A. Oswald, in Ref. 7, p. 53.
10. H. S. Makowski, P. K. Agarwal, R. A. Weiss, and R. D. Lundberg, *Polym. Prepr.*, **20**(2), 281 (1979).
11. R. M. Neumann, W. J. MacKnight, and R. D. Lundberg, *Polym. Prepr.*, **19**(2), 298 (1978).
12. B. Siadat, R. D. Lundberg, and R. W. Lenz, *Polym. Eng. Sci.*, **20**, 530 (1980).
13. P. K. Agarwal, H. S. Makowski, and R. D. Lundberg, *Macromolecules*, **13**, 1679 (1980).
14. I. Duvdevani, R. D. Lundberg, and J. R. Alonzo, *Proc. 37th ANTEC, Soc. Plast. Eng.*, **25**, 628 (1979).
15. P. K. Agarwal, I. Duvdevani, and R. D. Lundberg, *Proc. 39th ANTEC, Soc. Plast. Eng.*, **27**, 835 (1981).
16. J. J. Maurer and G. D. Harvey, *Proc. 11th NATAS Conf.*, **2**, 53 (1981).
17. J. J. Maurer, *Proc. 7th ICTA Conf.*, (1982), to appear.
18. R. A. Weiss, *Proc. 7th ICTA Conf.*, (1982), to appear.
19. H. S. Makowski, R. D. Lundberg, and G. Singhal, U.S. Pat. 3,870,841 (1975) (assigned to Exxon Research and Engineering Co.).
20. *Handbook of Chemistry and Physics*, 59th ed., CRC Press, 1978–1979, West Palm Beach, FL, p. B-183.

Received March 14, 1983
Accepted July 7, 1983